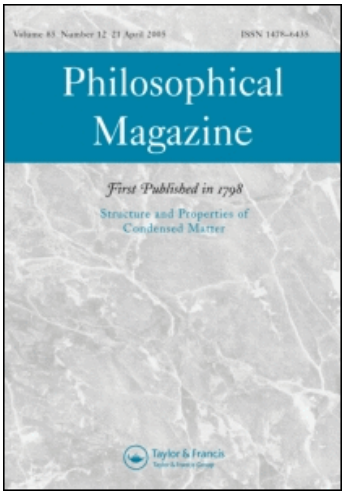

Philosophical Magazine
Publication details, including instructions for authors and subscription information:
http://www.informaworld.com/smpp/title~content=t713695589

GW correlation effects on plutonium quasiparticle energies: Changes in crystal-field splitting

A. N. Chantis [a]; R. C. Albers [a]; A. Svane [b]; N. E. Christensen [b]
[a] Theoretical Division, Los Alamos National Laboratory, Los Alamos, New Mexico, 87545, USA [b] Department of Physics and Astronomy, University of Aarhus, DK-8000 Aarhus C, Denmark

To cite this Article Chantis, A. N., Albers, R. C., Svane, A. and Christensen, N. E.'GW correlation effects on plutonium quasiparticle energies: Changes in crystal-field splitting', Philosophical Magazine, 89: 22, 1801 — 1811
To link to this Article: DOI: 10.1080/14786430902720960
URL: http://dx.doi.org/10.1080/14786430902720960

Philosophical Magazine
Vol. 89, Nos. 22–24, 1–21 August 2009, 1801–1811

Taylor & Francis
Taylor & Francis Group

GW correlation effects on plutonium quasiparticle energies: Changes in crystal-field splitting

A.N. Chantis[a]*, R.C. Albers[a], A. Svane[b] and N.E. Christensen[b]

[a]*Theoretical Division, Los Alamos National Laboratory, Los Alamos, New Mexico, 87545, USA;* [b]*Department of Physics and Astronomy, University of Aarhus, DK-8000 Aarhus C, Denmark*

(*Received 4 November 2008; final version received 4 January 2009*)

We present results for the electronic structure of plutonium by using a recently developed quasiparticle self-consistent GW method (QSGW). We consider a paramagnetic solution without spin-orbit interaction as a function of volume for the face-centred cubic (fcc) unit cell. We span unit-cell volumes ranging from 10% greater than the equilibrium volume of the δ phase to 90% of the equivalent for the α phase of Pu. The self-consistent GW quasiparticle energies are compared to those obtained within the Local Density Approximation (LDA). The goal of the calculations is to understand systematic trends in the effects of electronic correlations on the quasiparticle energy bands of Pu as a function of the localisation of the *f* orbitals. We show that correlation effects narrow the *f* bands in two significantly different ways. Besides the expected narrowing of individual *f* bands (flatter dispersion), we find that an even more significant effect on the *f* bands is a decrease in the crystal-field splitting of the different bands.

Keywords: plutonium; electron correlations; GW approximation; first-principles electronic structure

1. Introduction

Much of our modern understanding of electronic correlations in narrow-band systems has derived from many-body treatments of model Hamiltonian systems such as the Hubbard model and the Anderson model. For example, with respect to plutonium in particular, dynamical mean-field theory (DMFT) approaches have been very useful in elucidating the physics of the very strong correlations in this material (see, for example, [1,2] and references therein). Nonetheless, these calculations are not first principles, and most of the physics comes from the model part of the Hamiltonian rather than the band-structure part of the calculations. Thus, it is important to better understand the multi-orbital and hybridisation effects in more realistic electronic-structure approaches that are less model dependent. The GW method is our best modern tool for examining these effects, because it includes correlation effects beyond those of conventional

*Corresponding author. Email: achantis@lanl.gov

ISSN 1478–6435 print/ISSN 1478–6443 online

DOI: 10.1080/14786430902720960
http://www.informaworld.com

local-density approximation (LDA) band-structure techniques, and yet is still first-principles.

In this paper, we study correlation effects of fcc Pu as a function of volume. Our goal is not to specifically elucidate the correlation physics of Pu itself, since the GW approach is a low-order approximation and cannot treat the very strong correlations of the δ phase of Pu. Rather, we wish to use the volume dependence to tune the material from high atomic density (high pressure), where correlations can be greatly reduced due to the large hybridisation between the Pu f orbitals, to low atomic densities (where the pressure would actually be negative), where the correlations effects are very strong. By following this procedure, we can understand how correlations modify the properties of a material *within the GW approximation*. When the correlations become strong, it is certainly the case that higher-order approximations like DMFT are necessary to accurately describe the material. Nonetheless, since GW is probably the correct starting point for such types of more sophisticated approaches, it is useful to understand what happens to the electronic structure of the material within the GW approximation as a function of the strength of the correlation effects, and, in particular, their effects on shifts in quasiparticle energies, which is what GW is best at representing.

In order to focus more specifically on the effects of correlations, we ignore one significant aspect of the electronic structure, viz., the spin-orbit coupling, even though this is important for a detailed comparison with experiment. Spin-orbit coupling mainly shifts f states around in energy, but at the same time adds to the complexity of the individual f bands, hence tending to hide some of the correlation physics in a bewildering array of bands. Spin-orbit effects can easily be added in when a more accurate comparison with experiment is desired (as was done for an earlier paper on less correlated α-uranium [3]).

For the same reasons, we also ignore well-known large changes in crystal structure of Pu metal with volume, and present calculations only for the simple fcc crystal structure as a function of volume. We study a range of Pu atomic volumes, extending from well below that pertinent to the ground state α phase to well above that of the high-temperature δ phase. The actual crystal structure of α-Pu is a complicated monoclinic structure with 16 atoms per unit cell, while δ-Pu has the fcc structure. Since δ-Pu is well known to be a strongly correlated-electron metal, while α-Pu appears to be reasonably well treated by conventional band-structure methods, we believe that our range of volumes corresponds to tuning the correlation effects between weak to moderate (small volumes) to strongly correlated (large volumes).

In the calculations to be presented in the following, we mainly focus on changes in the effective bandwidth of the f states in Pu. We will show that crystal-field effects are actually a more important factor in determining this bandwidth than the expected change in dispersion (flattening of the bands).

2. Method

The GW approximation can be viewed as the first term in the expansion of the non-local energy-dependent self-energy $\Sigma(\mathbf{r}, \mathbf{r}', \omega)$ in the screened Coulomb interaction W. From a more physical point of view, it can be interpreted as a dynamically screened

Hartree–Fock approximation plus a Coulomb-hole contribution [4]. It is also a prescription for mapping the non-interacting Green function onto the dressed Green's function: $G^0 \rightarrow G$. This prescription can be described as follows: from the Hamiltonian,

$$H_0 = -\nabla^2 + V_{\text{eff}}(\mathbf{r}, \mathbf{r}'), \tag{1}$$

(we use atomic Rydberg units: $\hbar = 2m = e^2/2 = 1$, where m and e are the mass and charge of the electron) $G^0 = (\omega - H_0)^{-1}$ may be constructed. Often G^0 is calculated from the LDA eigenvalues and eigenfunctions; however, there is no formal restriction for how to choose the initial starting point G^0. Then, using the Random Phase Approximation (RPA) [4], we can construct the polarisation function D and screened Coulomb interaction W as

$$D = -iG^0 \times G^0 \tag{2}$$

and

$$W = u \times \frac{1}{1 - uD}, \tag{3}$$

where u is the bare Coulomb interaction. The new Green's function is defined as

$$G = \frac{1}{\omega - (-\nabla^2 + V^{\text{ext}} + V^{\text{H}} + \Sigma)}, \tag{4}$$

where V^{ext} is the potential due to ions (Madelung) and V^{H} is the Hartree potential

$$V^{\text{H}}(\mathbf{r}) = 2 \int \mathrm{d}\mathbf{r}' \frac{n(\mathbf{r}')}{|\mathbf{r} - \mathbf{r}'|}. \tag{5}$$

The single-particle density $n(\mathbf{r})$ is calculated as $n(\mathbf{r}) \sim \int_{-\infty}^{\infty} \mathrm{d}\omega G^0(\mathbf{r}, \mathbf{r}, \omega) e^{i\omega\delta}$.

In addition to this mapping of $G^0 \rightarrow G$, one can also generate an excellent effective potential from G that makes it possible to approximately do the inverse mapping of $G \rightarrow G^0$ [6]. QSGW is a method of specifing this (nearly) optimal mapping of $G \rightarrow G^0$, so that $G^0 \rightarrow G \rightarrow G^0 \rightarrow \ldots$ can be iterated to self-consistency [6,8]. At self-consistency, the quasiparticle energies of G^0 coincide with those of G. The QSGW method is a self-consistent perturbation theory, where the self-consistency condition is constructed to minimise the size of the perturbation. The QSGW method is parameter-free, and independent of basis set as well as the LDA starting point [5,6,8]. We have previously shown that QSGW reliably describes a wide range of *spd* [6,7,9–11], and rare-earth [12] systems. We have also applied the method to calculate the electronic structure of α-uranium [3].

Our version of the QSGW method is based upon the Full Potential Linear Muffin Tin Orbital (FP-LMTO) method [13], which makes no approximation for the shape of the crystal potential. The smoothed LMTO basis [5] includes orbitals with $l \leq l_{\max} = 6$; both $7p$ and $6p$ as well as both $5f$ and $6f$ are included in the basis. The $6f$ orbitals are added as a local orbital [5], which is confined to the augmentation sphere and has no envelope function. The $7p$ orbital is added as a kind of extended 'local orbital', the 'head' of which is evaluated at an energy far above Fermi level [5] and instead of making the orbital vanish at the augmentation radius a smooth Hankel

'tail' is attached to the orbital. The 7*p* and 6*f* orbitals are necessary to obtain an accurate description of high-lying bands, which are important for the accuracy of the polarisation function in Equation (2). For our calculations we use the fcc Pu lattice with the following lattice constants: $a = 4.11$ Å (which corresponds to 90% of the α-Pu equilibrium volume), 4.26 Å (at the α-Pu equilibrium volume), 4.64 Å (at the δ-Pu equilibrium volume) and 4.79 Å (at 110% of the δ-Pu equilibrium volume).

3. Results

In Figure 1, we compare the QSGW one-particle electronic structure of δ-Pu with the LDA band-structure results. The spin-orbit interaction is not included in this calculation. The Mulliken weights of the *f* orbitals are presented in red (dark grey), of the *s* orbitals in black and of the *d* orbitals in blue (light grey). In both cases, the narrow bands located between −2 and 2 eV are predominantly due to seven 5*f* orbitals. At the Γ point, they are split by the cubic crystal field into one non-degenerate and two three-fold degenerate states. This degeneracy is reduced at general k-points in the Brillouin zone. The lowest dispersive band centred around −4 eV has primarily *s* character and the unoccupied bands above 2 eV are mainly due to *d* orbitals. At the Γ point, the five *d* states are split by the cubic crystal field into one two-fold degenerate and one three-fold degenerate state. The *sdf* hybridisation along the symmetry directions presented in Figure 1, is generally very weak except for near the *X* point along the $\Gamma - X$ direction, where there is very strong *sd* and *df* hybridisation for some of the *d* and *f* branches. The degree of the hybridisation is very similar in both the LDA and QSGW calculations, as is the centre of all of the bands. The largest visible change is a significant narrowing of the 5*f*-band complex. This effect has two components: first, the crystal-field splitting of the *f* bands is significantly reduced in QSGW; second, the bandwidth of each individual *f* branch (band) is also reduced in QSGW. The total effect appears as an overall narrowing of the total density of states (DOS) around the Fermi level (see Figure 1c). In addition, since the area under the curve is proportional to the number of 5*f* states, which remains constant, the amplitude of the quasiparticle peaks is also higher in QSGW. For example, the total DOS at the Fermi level in QSGW is 23 states/eV while in LDA it is 9 states/eV.

The partial DOS is presented in Figure 2. In both calculations the partial 5*f* DOS is concentrated in a narrow energy interval around E_F. The partial *s* DOS is mainly located in the occupied energy spectrum between −5 eV and E_F, and the *d* bands are spread in a wide energy interval in both the unoccupied and occupied part of the spectrum with a few pronounced peaks at various energies. Overall, the QSGW and LDA *s* and *d* peaks are located at the same energies, with the exception of the narrow peaks around E_F, in which case the QSGW are visibly shifted closer to E_F. In this region, these bands can be highly hybridised with the *f* states, and thus these shifts reflect the band narrowing of the *f* states. The bottom of the *s* and *d* bands relative to the position of *f* band is approximately at the same energy location in QSGW and LDA. The *f* occupation changes in QSGW from its LDA value of 5.06 to 4.85 states. A similar reduction was observed in our calculations for α-uranium [3].

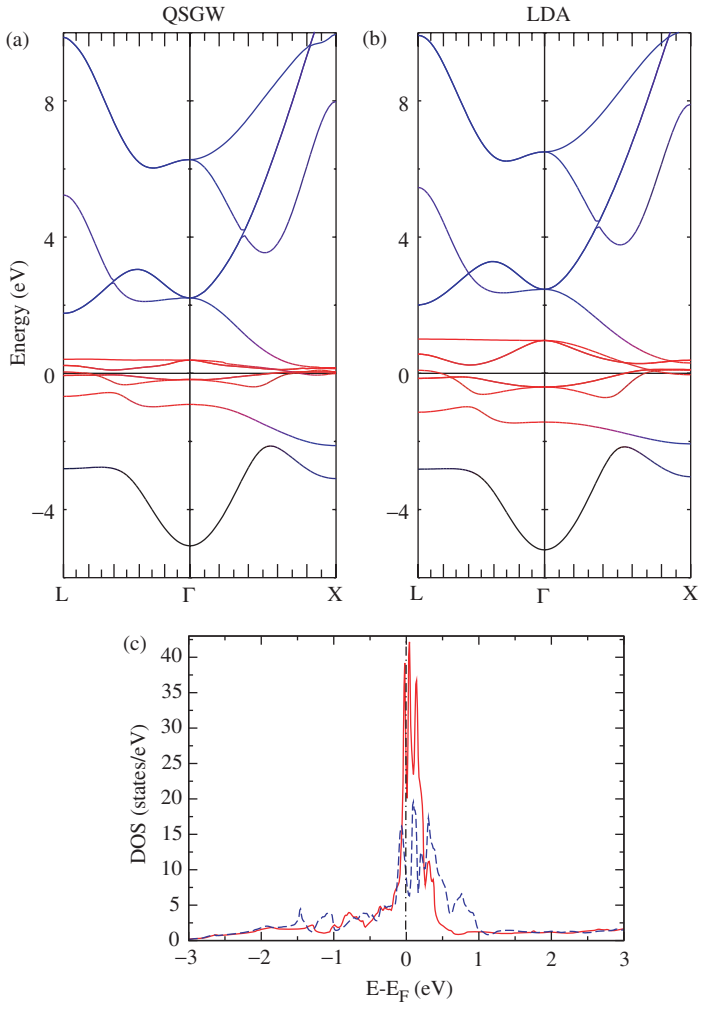

Figure 1. (Colour online). (a) The QSGW energy bands (or quasiparticle energies) for δ-Pu along two symmetry directions (left panel), compared to (b) the LDA energy bands (right panel); the Mulliken weights of the *f* orbitals are presented in red (dark grey), for *s* orbitals in black and for *d* orbitals in blue (light grey). (c) Comparison of the total density of states (DOS) for QSGW, red (dark grey) solid line, and LDA, blue (light grey) dashed line. The Fermi energy is set at zero.

In Figure 3, we present the band structures side by side for two different fcc volumes. On the left side is the band structure and partial *s* and *d* DOS for the α volume (weakly correlated) and on the right side is the band structure and partial *s* and *d* DOS for the δ volume (strongly correlated). In all cases, the red solid lines (colour online only) represent the QSGW results and the dashed blue lines (colour online only) show the LDA results. Two major effects are seen in this plot: (1) the *f* bands narrow considerably with expanded volume, and (2) there is a similar effect

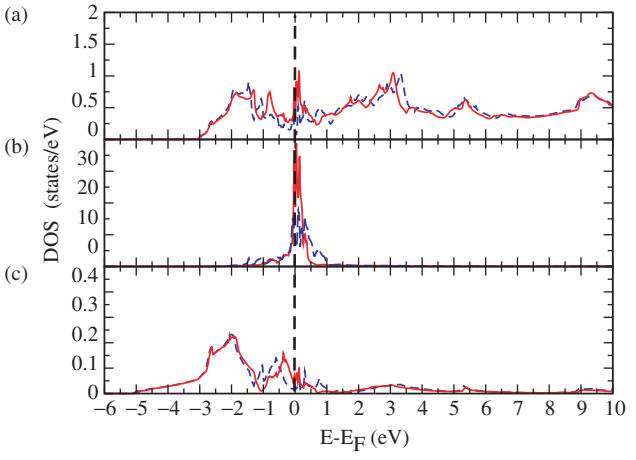

Figure 2. (Colour online). Comparison of QSGW, red (dark grey) solid line, and LDA, blue (light grey) dashed line, partial DOS for (a) the *d* orbitals, (b) the *f* orbitals, and (c) the *s* orbitals.

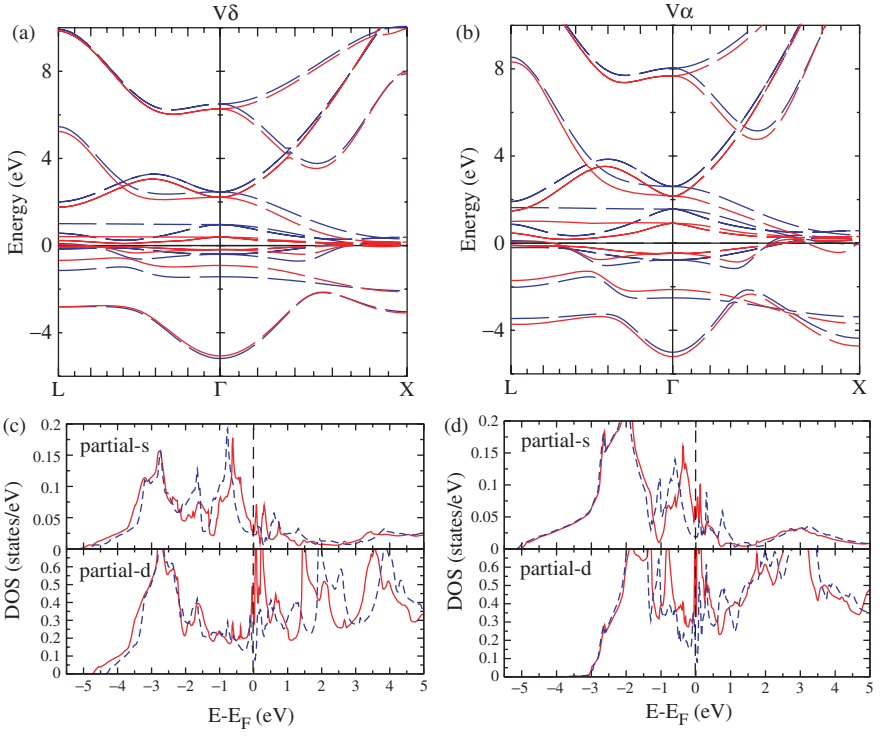

Figure 3. (Colour online). Comparison of the QSGW, red (dark grey) solid line, and LDA, blue (light grey) dashed line, band structure. On the left side are the energy bands for the more weakly correlated case for $a = 4.26$ Å (equivalent to the density of atoms for the α-Pu equilibrium volume), and on the right side the more strongly correlated case of $a = 4.64$ Å (the δ-Pu equilibrium volume).

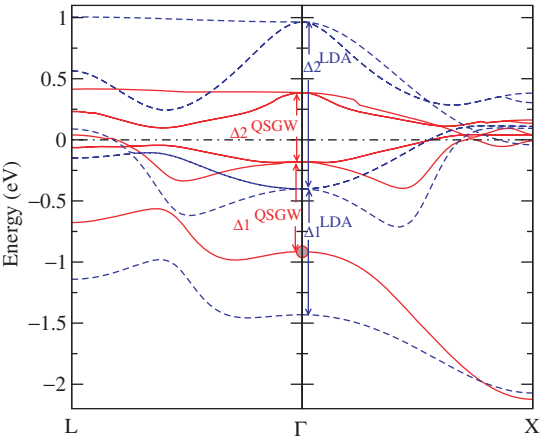

Figure 4. (Colour online). Comparison of QSGW, red (dark grey) solid line, and LDA, blue (light grey) dashed line, energy bands along two symmetry directions. The magnitudes of crystal field splittings Δ_1, Δ_2 are 1.02, 1.37 eV in LDA and 0.73, 0.57 eV in QSGW. Δ_2 is reduced significantly in the QSGW calculation. For the 5*f* state at the Γ point, marked with a large dot, in Figure 5, we present the energy dependence of the self-energy and calculated spectral function $A(\omega)$.

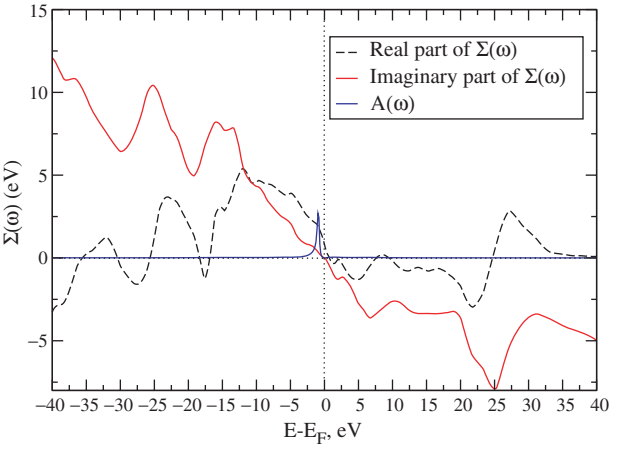

Figure 5. The energy dependence of the real and imaginary part of the self-energy together with the spectral function for the quasiparticle at $\mathbf{k} = (0, 0, 0)$ and $E_0 = -0.917$ eV.

on the *d* bands (notice the downward shift of the bands at the highest energy as one goes from the α to the δ volume).

To examine band narrowing effects in more detail, in Figure 4, we expand the view of the 5*f* bands. Also, in Figure 5, we show the self-energy and spectral function for one of the QSGW 5*f* states. Despite the complicated energy dependence of the real and imaginary parts it appears that the state is described perfectly well by Landau's Fermi liquid theory. The imaginary part of the self-energy goes through zero at E_F and the spectral function has a *single* well-defined peak centred at the

Table 1. The bandwidth of Pu 5*f* bands along $L-\Gamma$ and $\Gamma-X$ symmetry directions. The bandwidth is defined as the difference between the maximum and the minimum energy of a particular band along the direction. The width is given in eV.

	$L-\Gamma$	$\Gamma-X$
A_2 LDA	0.48	0.64
A_2 QSGW	0.43	1.21
T_1 LDA	0.71	0.83
T_1 QSGW	0.38	0.44
T_2 LDA	0.77	1.02
T_2 QSGW	0.32	0.45

QSGW eigenvalue. There are no other pronounced features in the energy dependence of the spectral function. This is representative of all 5*f* states. So the 5*f* states within the QSGW theory are well-defined quasiparticles with very large lifetime around E_F; the QSGW eigenvalues coincide with the quasiparticle energy. Therefore, our discussion is focused on the effects of electron correlations on the QSGW eigenvalues. At the Γ point, the *f* orbitals are split by the cubic crystal field into a non-degenerate state A_2 and two three-fold degenerate states, T_1 and T_2. The splitting, Δ_1, between the non-degenerate state and the lowest of the three-fold degenerate states is 1.02 eV in LDA and 0.73 eV in QSGW. The splitting, Δ_2, between the two three-fold degenerate states is equal to 1.37 eV in LDA, but only 0.57 eV in QSGW. This significant reduction of the crystal field splitting in QSGW is the major part of the band narrowing observed in the DOS in Figure 1. Another important aspect is the reduction of the width of each individual *f* band. In Table 1, we present the values of the bandwidth of Pu 5*f* bands along $L-\Gamma$ and $\Gamma-X$ symmetry directions. The bandwidth is defined as the difference between the maximum and the minimum energy of a particular band along the direction. In all cases, the bandwidth is reduced significantly in QSGW. The A_2 band along $\Gamma-X$ is a striking exception from this rule. As we show in Figure 6, this band strongly hybridises with the *d* states. At the Γ point it is 100% *f* but at the *X* point, it is predominately *d*. All the other bands shown in Figure 4 remain 80–100% *f* throughout the symmetry directions shown in the figure. This explains the anomalous change in the width of this band for this particular direction. From Figure 3, it is evident that, while in QSGW the width of the *f* bands are significantly reduced, the width of *d* bands are practically the same as for LDA. The A_2 band at the Γ point has mainly *f* character and therefore moves upward from its LDA position due to the significant reduction of the *f* crystal field in QSGW, but at the *X* point it mainly has *d* character and therefore remains approximately at its LDA position (only slightly lower due to the slight downward shift of the centre of *d* band in QSGW). The cumulative effect is that in QSGW this band is stretched. In Tables 2 and 3, we show the values for the crystal field splitting of 5*f* bands and *f* bandwidths along $L-\Gamma$ for several volumes of the unit cell. The bandwidth and crystal field splitting of all bands is reduced as we move from the lower to higher volume case.

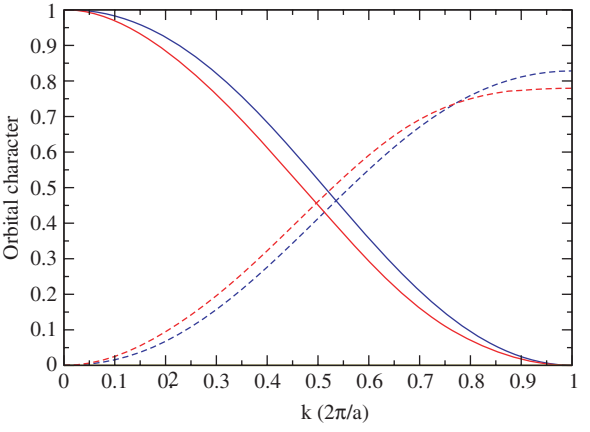

Figure 6. (Colour online). QSGW, red (dark grey) solid line, and LDA, blue (light grey) solid line *f*-orbital weight of the A_2 band along $\Gamma - X$ direction. Also shown is the QSGW, red (dark grey) dashed line, and LDA, blue (light grey) dashed line *d*-orbital weight of the A_2 band along the same direction.

Table 2. The crystal field splitting Δ_1 and Δ_2 of Pu 5*f* states at the Γ point. The QSGW values for the splitting are significantly smaller than those of the LDA calculation. The energy splitting is given in eV.

	$0.9\ V_\alpha$	V_α	V_δ	$1.1\ V_\delta$
Δ_1^{LDA}	2.14	1.75	1.02	0.84
Δ_1^{QSGW}	2.09	1.67	0.73	0.51
Δ_2^{LDA}	2.86	2.33	1.37	1.11
Δ_2^{QSGW}	1.96	1.36	0.57	0.41

Table 3. The bandwidth of Pu 5*f* bands along $L - \Gamma$ symmetry directions for different volumes of the unit cell. The bandwidth is defined as the difference between the maximum and the minimum energy of a particular band along the direction. We also provide the full width at half maximum (FWHM) of the broadened *f*-partial DOS shown in Figure 7. The width is given in eV.

	$0.9\ V_\alpha$	V_α	V_δ	$1.1\ V_\delta$
A_2 LDA	1.42	1.0	0.48	0.37
A_2 QSGW	1.23	0.94	0.43	0.30
T_1 LDA	1.38	1.15	0.71	0.6
T_1 QSGW	1.17	0.86	0.38	0.28
T_2 LDA	1.62	1.29	0.77	0.63
T_2 QSGW	1.30	0.84	0.32	0.23
FWHM LDA	1.28	1.09	0.78	0.72
FWHM QSGW	0.79	0.63	0.39	0.34

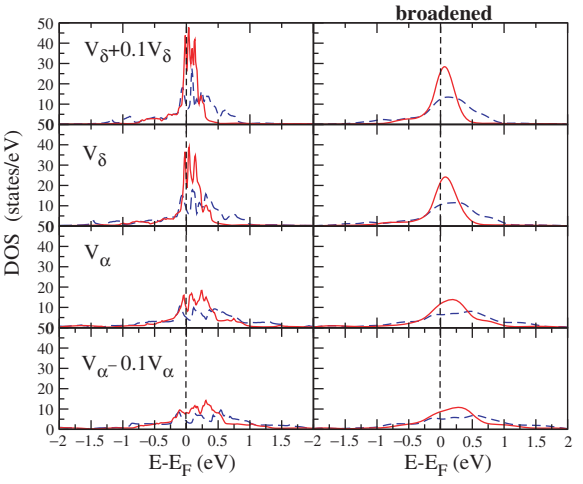

Figure 7. (Colour online). The QSGW and LDA *f*-partial DOS for four different volumes. The panels on the right side show the corresponding DOS on the left panel broadened with a Gauss function.

This is a result of the reduction of the *f* band relative to the extension in the crystal. It is also seen that the QSGW crystal field splittings and bandwidths for *f* orbitals are always smaller than in LDA. We have also considered the bandwidth of the entire 5*f* band complex. To do this, we have applied a Gaussian broadening on the partial-*f* DOS (Figure 7). In this case, the 5*f* band complex appears like a single large peak. We can define the width of this band as the full width at half maximum (FWHM) of the peak. This is also presented in Table 3. It is evident that in both calculations the width is reduced as the volume increases. The rate of reduction is the same in both calculations. But the QSGW FWHM is always significantly smaller than the LDA. Therefore, we conclude that, in QSGW, the *f* orbitals contract due to the more accurate treatment of correlations. On the other hand, the *s* and *d* bands are very itinerant and are therefore already described accurately at the level of the LDA treatment of correlations.

4. Conclusions

In conclusion, we have applied QSGW theory to *δ*-plutonium as a function of volume in order to systematically understand the effects of electronic correlation on the band narrowing of the *f* bands. Unlike the conventional Hamiltonian model treatment of strongly correlated systems, our approach is first principles and independent of any choice of model parameters, and hence provides a unique opportunity to examine the effect of electron correlations on the quasiparticle band structure as a function of *f*-orbital localisation. In this way, we have demonstrated that QSGW and LDA predictions for the *s* and *d* electron subsystems are quite similar. This is because these electrons are very itinerant and therefore their description lies within the validity of LDA. However, the QSGW

5*f* bands are much narrower than their LDA counterpart. We believe that our results show for the first time, significant details of the band narrowing due to electron correlations that have not been previously studied. In particular, the QSGW calculations show that the major contribution to band narrowing is actually the reduction of the crystal-field splitting of 5*f* states as compared to effects from a reduction in dispersion (flattening of the individual bands). This is a significant change in the character of the 5*f* states and suggests the importance of using GW approaches as input to more sophisticated correlation approaches such as dynamical mean-field theories (DMFT).

Acknowledgements

This work was carried out under the auspices of the National Nuclear Security Administration of the US Department of Energy at Los Alamos National Laboratory under Contract No. DE-AC52-06NA25396. ANC would like to thank Mark van Schilfgaarde and Takao Kotani for informative discussions.

References

[1] C.A. Marianetti, K. Haule, G. Kotliar et al., Phys. Rev. Lett. 101 (2008) p.056403.
[2] J.H. Shim, K. Haule, S. Savrasov et al., Phys. Rev. Lett. 101 (2008) p.126403.
[3] A.N. Chantis, R.C. Albers, M.D. Jones et al., Phys. Rev. B 78 (2008) p.081101.
[4] L. Hedin, J. Phys. Condens. Matter 11 (1999) p.R489.
[5] M. van Schilfgaarde, T. Kotani and S.V. Faleev, Phys. Rev. B 74 (2006) p.245125.
[6] M. van Schilfgaarde, T. Kotani and S. Faleev, Phys. Rev. Lett. 96 (2006) p.226402.
[7] S.V. Faleev, M. van Schilfgaarde and T. Kotani, Phys. Rev. Lett. 93 (2004) p.126406.
[8] T. Kotani, M. van Schilfgaarde and S.V. Faleev, Phys. Rev. B 76 (2007) p.165106.
[9] T. Kotani, M. van Schilfgaarde, S.V. Faleev et al., J. Phys. Condens. Matter 19 (2007) p.365236.
[10] A.N. Chantis, M. Cardona, N.E. Christensen et al., Phys. Rev. B 78 (2008) p.075208.
[11] A.N. Chantis, M. van Schilfgaarde and T. Kotani, Phys. Rev. Lett. 96 (2006) p.086405.
[12] A.N. Chantis, M. van Schilfgaarde and T. Kotani, Phys. Rev. B 76 (2007) p.165126.
[13] M. Methfessel, M. van Schilfgaarde and R.A. Casali, in *Electronic Structure and Physical Properties of Solids: The Uses of the LMTO Method*, H. Dreysse ed., Lecture Notes in Physics Vol. 535. Springer-Verlag, Berlin, 2000.